

## Pulse Width Modulation based Soft switched Flyback dc/dc Converter for Improved System Performance

Dr. Anasraj R  
Associate Professor,  
Government Engineering College,  
Thrissur, Kerala, India

Jithin P R  
M.Tech student  
Government Engineering College,  
Thrissur, Kerala, India

### Abstract

*This paper presents a soft switched pulse width modulation (PWM) based flyback dc/dc converter using a soft switching auxiliary circuit. Compared to the conventional hard switching flyback converter, this soft switching PWM converter is more efficient since it has no additional conduction loss and current stress in the main switch. Constant switching frequency and low commutation losses are also the advantages of the proposed converter. Simulation results of the soft switched PWM converter is validated in the hardware setup.*

### 1. Introduction

Modern technology continues to move towards smaller more densely packed board solutions. Higher component density places pressures on all parts of a design to either miniaturize components or build simpler solutions. One area that pushes toward smaller and more efficient designs is the power supply market. With the advent of more functional blocks and size constraints in new technology, the importance of good power design is essential. Increased amount of circuitry require more power along with various voltage levels. The processor may require 3V while another electronic subsystem requires 5V. At the same time, power solution must not waste too much energy during conversion since lost energy is converted to heat that must eventually be removed with large heat sink or fans. Thus the need to develop efficient, small, and simple power supplies has become a key goal of many power electronic designers. Component sizes have become smaller, but larger gains are made on the power side removing components from a design completely.

One area being pushed in both size and simplicity is the design of isolated power supply. The fastest growing telecommunication and computer systems require isolated power supplies. Isolated power

supplies require more external components and complexity to ensure true isolation and regulation of the output voltage. To meet the requirements of these applications, a number of pulse width modulation (PWM) topologies are commonly used to implement the isolated power supplies. These topologies include the full bridge, half bridge, push-pull, double switch, single switch forward and flyback topologies, which are listed in the sequence from high power level down to low power level. Each topology has unique properties which makes it best suited for a certain power level.

Flyback converters are isolated versions of buck-boost converters and are widely used in low to medium power applications. They are relatively simple and have very few components. PWM based soft switching flyback converters are high efficient extent versions of single switched flyback converters. This topology costs an additional active circuit.

The purpose of this active switch is to turn off the main switch at zero current and reduce the switching losses. In this paper an overview of the soft switching, mainly ZCS in flyback converter is presented. The principle of operation of the ZCS switching cell in a flyback converter is explained. A comparative study of ZCS PWM flyback over conventional flyback converter is presented and simulation results of the soft Switching PWM flyback converter are given along with experimental results [4-5]. The main drawback in simple soft switching circuits is

- 1) High conduction losses in the main switch.
- 2) Complex control circuits are required.
- 3) The current control mode cannot be used.
- 4) An additional winding in flyback transformer is required.

### 2. Softswitched Flyback Converter

In this topology a soft switching PWM flyback converter with a simple soft switching -PWM commutation cell has been introduced which can

overcome the problems with conventional soft switching and hard switching flyback converters [6]. In the proposed converter, all semiconductor devices are operated at ZCS turn-on and turn-off condition. The auxiliary circuit does not require a complex control circuit since the auxiliary switch and main switch in the circuit have a common ground.

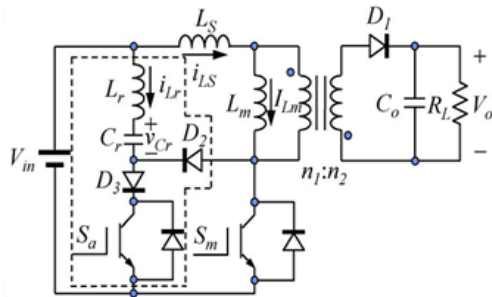


Fig. 1. Soft switched PWM-flyback converter

The circulating current for the soft switching flow through the auxiliary circuit, the conduction loss and current stress of the main switch are reduced. In addition, at constant frequency and with reduced commutation losses, the new ZCS-PWM flyback converter has no additional current stress and conduction losses in the main switch compared to its hard switching flyback converter counterpart.

### 3. Principle of Operation

The circuit of the soft switching PWM flyback converter with a PWM commutation cell is shown in Fig. 1. The power circuit consists of the main switch  $S_m$ , the secondary side rectifier diode  $D_1$ , and the flyback transformer with leakage inductance  $L_s$  and mutual inductance  $L_m$  with referred to the primary side. The ZCS-PWM switching cell is comprised of an auxiliary switch  $S_a$ , the resonant capacitor  $C_r$ , the resonant inductor  $L_r$ , and two auxiliary diodes  $D_1$  and  $D_2$ .

Operation of soft switching PWM flyback converter can be divided into two sections. When the main switch  $S_m$  is on,  $L_m$  and  $L_l$  are charged by the input voltage source and the converter operation is exactly similar to a conventional hard-switched flyback converter. The auxiliary switch  $S_a$  is turned on just before  $S_m$  is turned off resulting in resonance between  $L_r$  and  $C_r$ . The resonant capacitor  $C_r$  is discharged by the resonant current in the auxiliary circuit. When the resonant current reaches zero, the diode  $D_2$  seizes conduction and stops the flow of resonant current through auxiliary switch. The resonant current now flows through  $D_3$  and charges  $C_r$ .

When the resonant current through  $S_m$  reverses, the antiparallel diode  $D$  begins to conduct. When the antiparallel seizes conduction, the current through  $S_m$  is zero thereby creating a ZCS condition for  $S_m$  and  $S_a$ . The switches  $S_m$  and  $S_a$  are turned off during this time period. When the switches are turned off, the resonance between  $L_l$ ,  $L_r$ , and  $C_r$  begin, and the resonant current continues to charge  $C_r$ . The output rectifier  $D_1$  is forward biased and the magnetizing inductance current is transferred to the load. When the energy stored in  $L_r$  and  $L_l$  is transferred to  $C_r$ , the diode  $D_1$  commutates all of the magnetizing inductance current to the output until  $S_m$  is turned on in the next switching cycle. To simplify the circuit analysis, it is assumed that this converter is operated in steady-state and the some assumptions are made during the operation.

- 1) All the semiconductor devices and components are ideal.
- 2) The magnetizing inductor  $L_m$  is large enough to assume that the current  $I_{Lm}$  on the inductor  $L_m$  is constant and is much greater than that on the resonant inductor  $L_r$ .
- 3) The output voltage  $V_o$  is constant and ripple-free.
- 4) Before  $t = t_0$ , the resonant voltage  $v_{C_r}(t)$  equals  $VC_{r0}$ , the resonant current  $i_{Lr}(t)$  equals zero, and the current  $i_{L_s}(t)$  on the leakage inductor  $L_s$  equals zero.

The circuit has seven different modes of operation in one switching cycle. The seven dynamic equivalent circuits of the new ZCS-PWM flyback converter during one switching period are shown in Fig. 2. For analyses following parameters are defined:

$$n = \frac{n_1}{n_2} \quad (1)$$

$$nL = \frac{L_s}{L_r} \quad (2)$$

#### 3.1 Modes of Operation of the New ZCS-PWM Fly back Converter

**Mode A;** Before mode A, switches  $S_m$  and  $S_a$  are in off state. The energy stored in magnetizing inductor  $L_m$  is delivered to output filter capacitor  $C_o$ . when the main switch  $S_m$  turns on with ZCS this mode is initiated. The leakage inductor  $L_s$  charges linearly to output voltage  $V_o$  from zero to  $I_{Lm}$ . The stage ends when the current in

the leakage inductor  $L_s$  equal to  $I_{Lm}$  and diode  $D_1$  turns off. During this mode,

$$i_{Lr}(t) = 0 \tag{3}$$

$$i_{Ls}(t) = \frac{1}{L_s}(V_{in} + nV_o)(t - t_0) \tag{4}$$

$$V_{cr}(t) = V_{cro} \tag{5}$$

$$\Delta t_1 = \frac{I_{Lm} L_s}{V_{in} + nV_o} \tag{6}$$

**Mode B;** Operation of the converter at this mode is same as the operation of the conventional flyback converter. When the current  $i_{Ls}(t)$  in leakage inductor  $L_s$  reaches  $I_{Lm}$  and diode  $D_1$  turns off with ZCS, this stage is started. The magnetizing inductor  $L_m$  and the leakage inductor  $L_s$  are together charged linearly by source voltage  $V_{in}$ . During mode B

$$i_{Lr}(t) = 0 \tag{7}$$

$$i_{Ls}(t) = I_{Lm} \tag{8}$$

$$V_{cr}(t) = V_{cro} \tag{9}$$

$$\Delta t_2 = DT_s - \Delta t_1 \tag{10}$$

$D$  is the duty ratio and time of the main switch,  $T_s = 1/f_s$  is the switching period, and  $f_s$  is the switching frequency.

**Mode C;** when the auxiliary switch  $S_a$  is turned mode C is started. Initial value of resonant current  $i_{Lr}(t)$  is zero, auxiliary switch  $S_a$  can be turn-on at ZCS. The resonance of resonant inductor  $L_r$  and capacitor  $C_r$  is started in this mode. After reaching its peak value the resonant current  $i_{Lr}(t)$  decreases. The resonant voltage  $v_{Cr}(t)$  also increases. The magnetizing inductor  $L_m$  and the leakage inductor  $L_s$  are continuously charged by input voltage source  $V_{in}$ . when and the resonant voltage has reached its peak value the resonant current  $i_{Lr}(t)$  drops to null again this mode ends. The diode  $D_3$  is naturally closed.

$$i_{Ls}(t) = I_{Lm} \tag{11}$$

$$\Delta t_3 = \frac{\pi}{\omega r} \tag{12}$$

there are two resonant peaks given by,

$$I_{Lr,peak} = (V_{in} - V_o)/Z_o \tag{13}$$

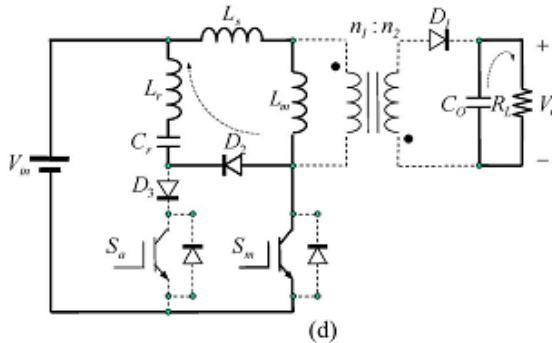
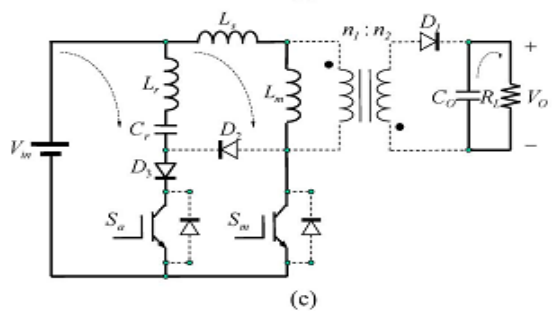
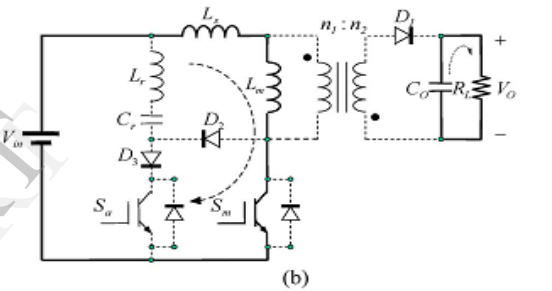
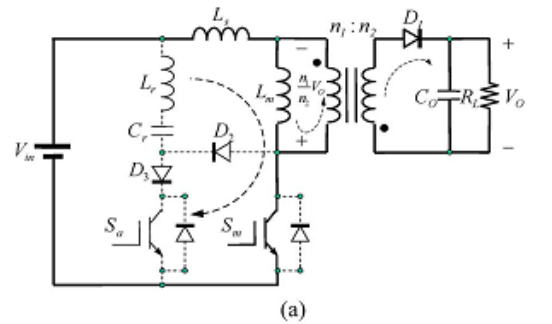
$$V_{Cr,peak} = 2V_{in} - V_{Cr0} \tag{14}$$

**Mode D;** In this mode, the resonant behavior in mode C is maintained, but the resonant route changes following  $V_{in}$ ,  $L_r$ ,  $C_r$ ,  $D_2$ , and  $S_m$ . The resonant voltage  $v_{Cr}(t)$  decreases and the resonant current  $i_{Lr}(t)$  rises toward its negative peak value. The magnetizing inductor  $L_m$  and the leakage inductor  $L_s$  are continuously charged by input voltage source  $V_{in}$

together. The stage is finished when the resonant current  $i_{Lr}(t)$  rises to  $-I_{Lm}$ . The resonant voltages  $v_{Cr}(t)$ , and the current  $i_{Ls}(t)$  in leakage inductor can be described as,

$$i_{Ls}(t) = I_{Lm} \tag{15}$$

$$\Delta t_4 = \frac{1}{\omega r} \sin^{-1} \frac{I_{Lm} Z_o}{V_{in} - V_{cro}} \tag{16}$$



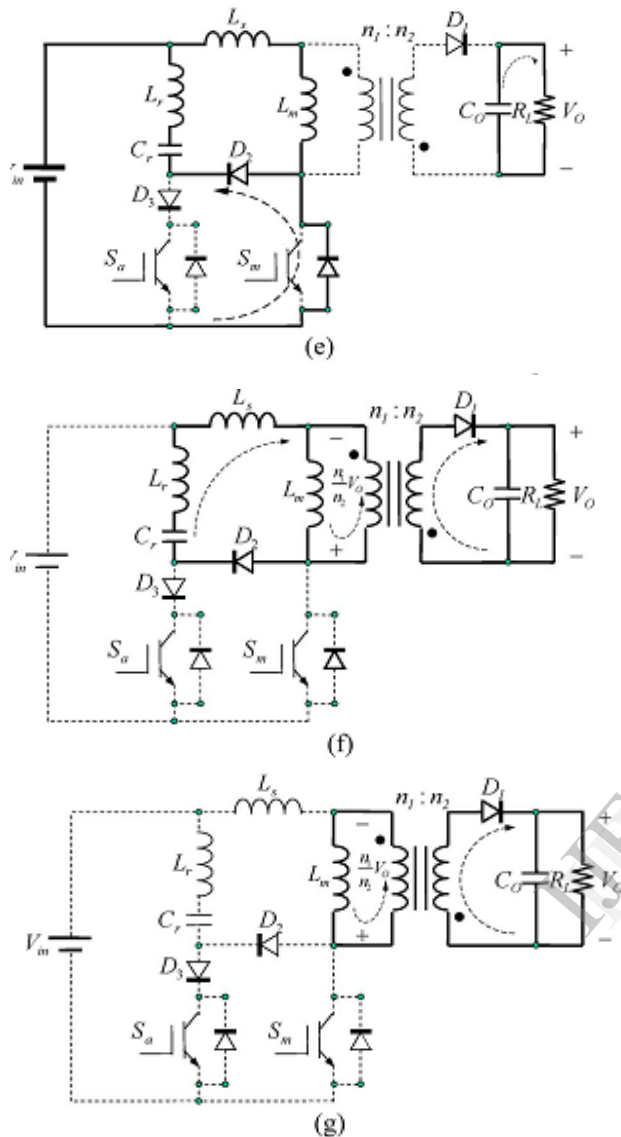


Fig. 2(a)-2(g) Modes of operation for Soft switching PWM Flyback converter

**Mode E;** At the end of previous mode the resonant current  $i_{Lr}(t)$  rises to  $-I_{Lm}$  and its flow path is changed by  $V_{in}$ ,  $L_r$ ,  $C_r$ ,  $D_2$ , and the antiparallel diode of  $S_m$ . Thus, no current flows through the main switch  $S_m$ . Furthermore, because the diode  $D_3$  is naturally closed, no current also flows through the auxiliary switch  $S_a$ . It is the best time to turn off the switches  $S_m$  and  $S_a$  under ZCS. The switches  $S_m$  and  $S_a$  are simultaneously turned off at ZCS and this mode is started. In this stage, the resonant operation in stage 3 is continuously maintained, while the resonant voltage  $v_{Cr}(t)$  continuously drops. The resonant current  $i_{Lr}(t)$  rises towards its negative peak value and then decreases. The magnetizing inductor  $L_m$  and the leakage inductor  $L_s$

are continuously charged by input voltage source  $V_{in}$  together. When the resonant current  $i_{Lr}(t)$  drops to  $-I_{Lm}$  again, the antiparallel diode of  $S_m$  is naturally closed and this stage is finished.

$$i_{Ls}(t) = \frac{I_{Lm}}{\omega T} \tag{17}$$

$$\Delta t_5 = \frac{\pi}{\omega r} - \Delta t_4 \tag{18}$$

**Mode F;** during this stage, the antiparallel diode of  $S_m$  is naturally closed and the diode  $D_1$  is turned on with ZCS. The energy stored in magnetizing inductor  $L_m$  begins to load through  $D_1$  and the voltage across the primary winding is fixed in  $-nV_o$ . Thus, another resonant route is formed by  $C_r$ ,  $L_r$ ,  $L_s$ ,  $nV_o$ , and  $D_2$ . The resonant voltage  $v_{Cr}(t)$  continuously decreases. The resonant current  $i_{Lr}(t)$  rises toward zero value and the current  $i_{Ls}(t)$  in the leakage inductor drops toward zero value. This stage ends when the energies stored in the resonant inductor  $L_r$  and the leakage inductor  $L_s$  are completely transferred to the resonant capacitor  $C_r$ .

**Mode G;** In this mode, the resonant current  $i_{Lr}(t)$  and the current  $i_{Ls}(t)$  in leakage inductor  $L_s$  is equal to zero, and the diode  $D_2$  is naturally turned off with ZCS. The energy stored in magnetizing inductor  $L_m$  is continuously loaded through  $D_1$ . This operating behavior is the same as the conventional PWM flyback dc/dc converter operating at turn-off state. The resonant current  $i_{Lr}(t)$ , resonant voltages  $v_{Cr}(t)$ , and the current  $i_{Ls}(t)$  in leakage inductor can be described as

$$i_{Lr}(t) = 0 \tag{19}$$

$$i_{Ls}(t) = 0 \tag{20}$$

$$v_{Cr}(t) = V_{Cr0} \tag{21}$$

$$\Delta t_7 = (1 - D)T_s - \sum_3^6 \Delta t_k \tag{22}$$

After mode G, the circuit operation returns to the first stage. The resonant voltage  $v_{Cr}(t)$  returns to the initial value  $V_{Cr0}$ . Both resonant current  $i_{Lr}(t)$  and  $i_{Ls}(t)$  return to zero. Therefore, the assumption previously made is proven to be valid.

#### 4. Simulation Results and Analysis

To characterize the soft-switching properties of the soft switching PWM flyback dc/dc converter, Matlab simulation has been done to the specifications listed below: And efficiency comparison between the Soft switching-PWM flyback dc/dc converter and conventional hard switching Flyback converter has been carried for same output rating.

- 1) Input voltage: 100 VDC,
- 2) Output voltage: 12 VDC,

- 3) Output power: 150 W maximum,
- 4) Switching frequency: 80 kHz

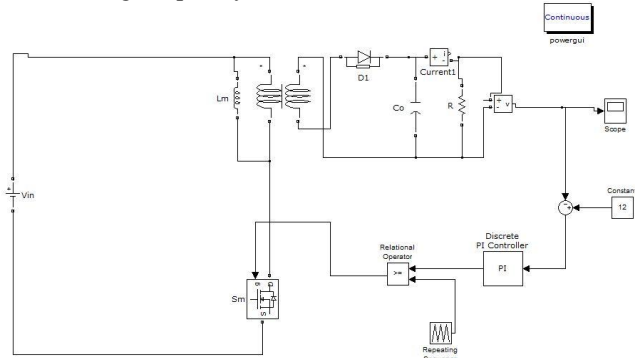


Fig.3 .Simulation Diagram of Conventional Flyback converter

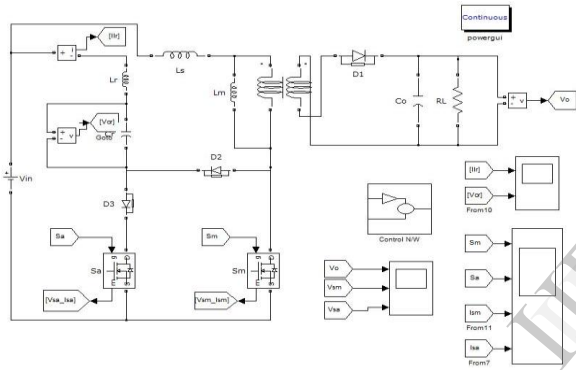


Figure 4(a) .Simulation Diagram of the ZCS-PWM flyback dc/dc converter.

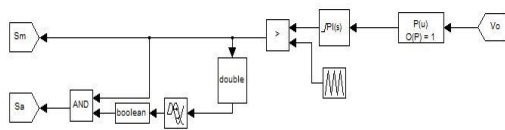


Figure 4(b) .Simulation Diagram of the control circuit ZCS-PWM flyback dc/dc converter

The simulink block model for the soft switching-PWM flyback converter and its control are shown in the figure 4(a) and 4 (b).The gate pulse to the main switch ( $S_m$ ) and auxiliary switch ( $S_a$ ) is shown in figure 5.The commutation phenomenon in the main switch  $S_m$ , auxiliary switch  $S_a$  shown respectively in figures 6(a) and 6(b). The simulation results demonstrate that ZCS

is achieved at constant frequency for both active switches ( $S_m$  and  $S_a$ ). It should be noted that the diode  $D_1$  and the main diode  $D_2$  were also softly.

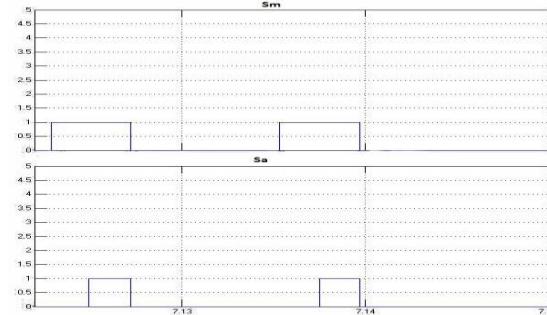


Fig. 5. Gate pulse to  $S_m$  and  $S_a$

Commutated under ZVS. The resonant current and resonant voltage in the auxiliary circuit is observed and shown in figure 7. Therefore, switching energy losses for this new ZCS-PWM flyback converter are practically zero. Both the Input and Output voltages waveforms are shown in Figure 8.

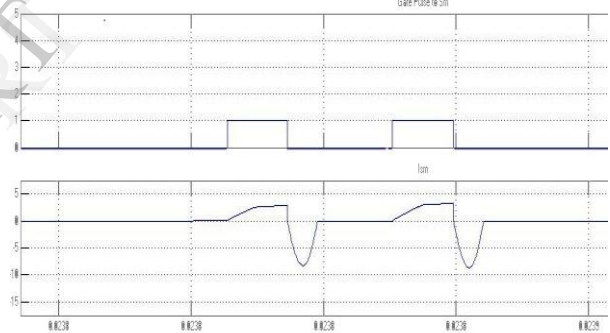


Fig.6(a). ZCS Operation of main switch  $S_m$

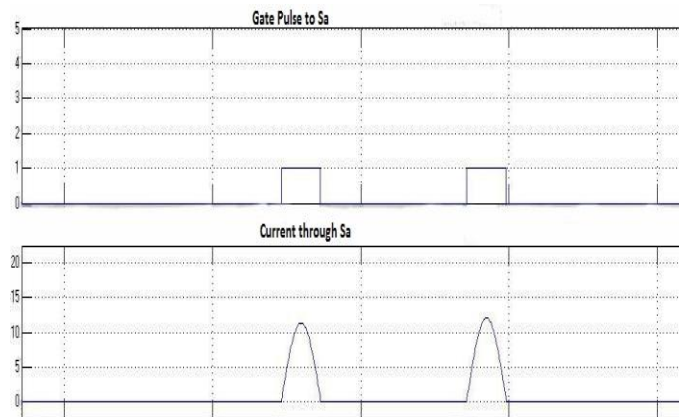


Figure 6(b). ZCS Operation of auxiliary switch  $S_a$

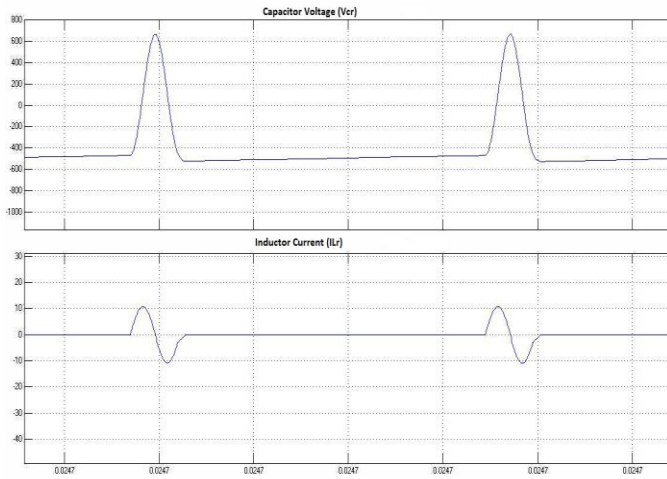


Fig. 7. Resonant capacitor voltage and resonant inductor Current

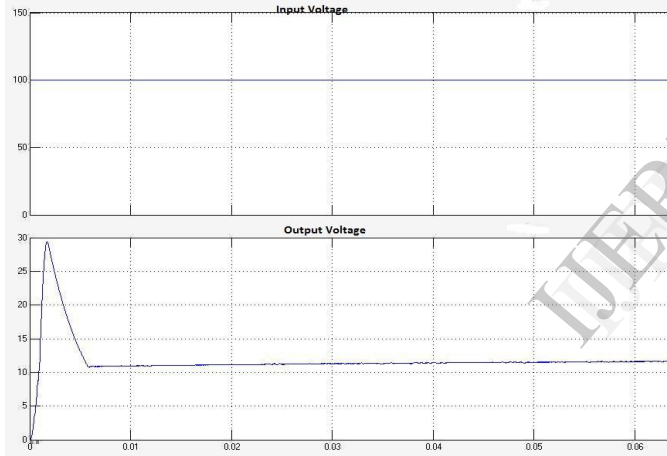


Fig.8. Input Voltage and Output Voltage Waveforms

**4.1 Efficiency comparison**

Efficiency comparison of soft switching PWM Flyback Converter with Conventional hard switching Flyback converter using MATLAB simulation is carried and performance is analysed .The efficiency measured at different power ratings with two topologies using Matlab simulation block for line and load regulation. The efficiency calculated based on the simulation results at load regulation for both softswitching PWM flyback converter and conventional flyback converter are tabulated in Table I and Table II respectively and the efficiency plotted has shown in Fig.9.Simulation results shows the proposed converter has better efficiency then conventional flyback converter throughout the operation.

**TABLE I**  
LOAD REGULATION EFFICIENCY OF CONVENTIONAL FLYBACK CONVERTER

Conventional Flyback converter					
V <sub>in</sub> (V)	P <sub>in</sub> (W)	V <sub>o</sub> (V)	R <sub>L</sub> (Ω)	P <sub>o</sub> (W)	Efficiency(%)
100	190.90	12	1	144	75.43
100	127.29	12	1.44	100	78.56
100	104.79	12	1.8	80	76.34
100	97.04	12	1.92	75	77.29
100	91.10	12	2.215	67.76	74.28
100	87.03	12	2.4	60	68.94
100	72.17	12	3	48	66.51

**TABLE II**

LOAD REGULATION EFFICIENCY OF PROPOSED FLYBACK CONVERTER

Soft Switched PWM- Flyback converter					
V <sub>in</sub> (V)	P <sub>in</sub> (W)	V <sub>o</sub> (V)	R <sub>L</sub> (Ω)	P <sub>o</sub> (W)	Efficiency(%)
100	190.90	12	1	144	75.43
100	127.29	12	1.44	100	78.56
100	104.79	12	1.8	80	76.34
100	97.04	12	1.92	75	77.29
100	91.10	12	2.215	67.76	74.28
100	87.03	12	2.4	60	68.94
100	72.17	12	3	48	66.51

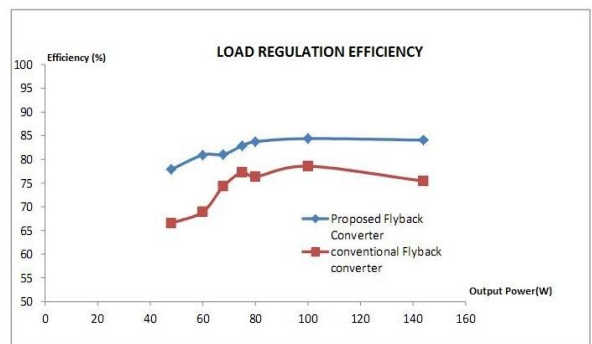


Fig.9. Efficiency at Load regulation

During the line regulation the input voltage varied between 30V to 100V by keeping constant load value. The efficiency during this operation has been tabulated in in Table III and Table IV. And the efficiency curve plotted in Fig.10 for both soft switching PWM Flyback converter and conventional hard switching Flyback converter. The absence of snubber circuits and low

conduction losses results in better efficiency to proposed soft switching flyback converter than hard switching flyback converter.

TABLE III  
LINE REGULATION EFFICIENCY OF CONVENTIONAL FLYBACK CONVERTER

Conventional Flyback converter					
$V_{in}$ (V)	$P_{in}$ (W)	$V_o$ (V)	$R_L$ ( $\Omega$ )	$P_o$ (W)	Efficiency(%)
30	132.77	12	1.44	100	75.32
45	132.29	12	1.44	100	75.59
55	135.08	12	1.44	100	74.03
70	131.25	12	1.44	100	76.18
85	131.75	12	1.44	100	75.90
100	131.43	12	1.44	100	76.09

TABLE IV  
LINE REGULATION EFFICIENCY OF PROPOSED FLYBACK CONVERTER

Soft Switched PWM- Flyback converter					
$V_{in}$ (V)	$P_{in}$ (W)	$V_o$ (V)	$R_L$ ( $\Omega$ )	$P_o$ (W)	Efficiency (%)
30	119.66	12	1.44	100	83.57
45	119.5	12	1.44	100	83.68
55	120.21	12	1.44	100	83.19
70	119.01	12	1.44	100	84.02
85	118.31	12	1.44	100	84.52
100	118.2	12	1.44	100	84.58

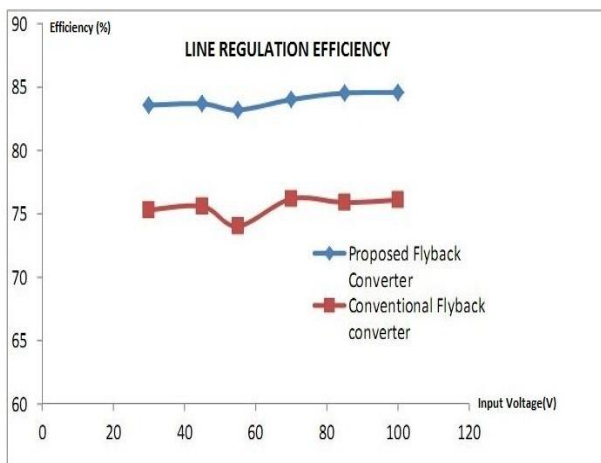


Fig.9. Efficiency at Line regulation

### 5. Experimental Results

The circuit has designed for output voltage of 12V and the components used are

- Active Switches Sa,Sb(IGBT) - FGA20S120M
- Diode D2,D3 – uf4007,D1-AN5209
- Resonant Capacitor (Cr)- 20nf
- Resonant Inductor(Lr)-45uH,
- Leakage Inductance(Ls)- 80uH,
- Magnetizing Inductor(Lm)-800uH
- Flyback transformer with turns 100:30
- Output capacitor (Co) = 470uF
- 4N26 opto coupler is used for f.b output voltage and TLP250 is used for the gate driver circuit
- dsPIC30F2010 used for control circuit

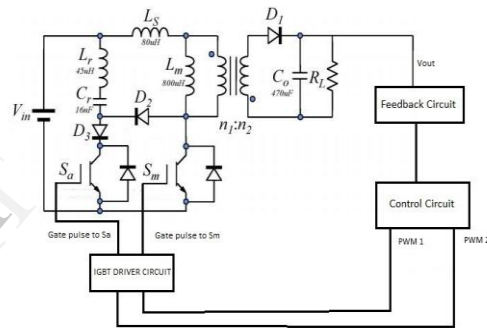


Fig.10. Hardware circuit

dsPIC30F2010 is used to generate the control signal. 3V regulated voltage supply for dsPIC is generated by using LM317 regulator.

Hardware for the ZCS PWM flyback converter with a ZCS PWM commutation cell has implemented and the performance of the new converter analyzed at load and line regulation.

The converter gives a constant output voltage for a range of input voltage variations and load variations. The ZCS operation at switches is also noted. This soft switching technique improves the efficiency of the converter. DsPIC30F2010 is used in the control circuit to generate PWM signal for the main and active switches. The PWM signal from control circuit fed to IGBT gate driver circuit. TLP 250 optocoupler is used for the driver circuit. Output feedback is taken using optocoupler 4N26

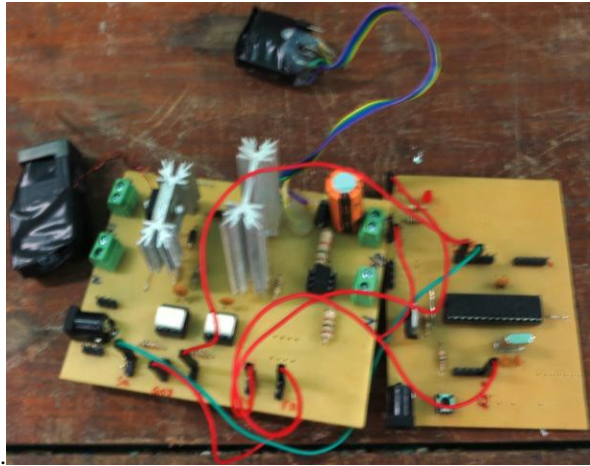


Fig.11. Experimental Setup

The PWM signal to Switches  $S_m$  and  $S_a$  are shown in figure 12. The signals are generated at 80KHz frequency. 12V output from the converter is shown in figure 20 and ZCS operation in  $S_a$  and  $S_b$  are given in figure 21 and 22 respectively.

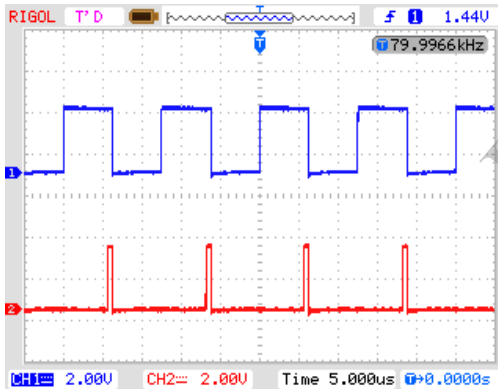


Fig.12. PWM Signal generated from control circuit



Fig.13. Regulated output voltage of the converter

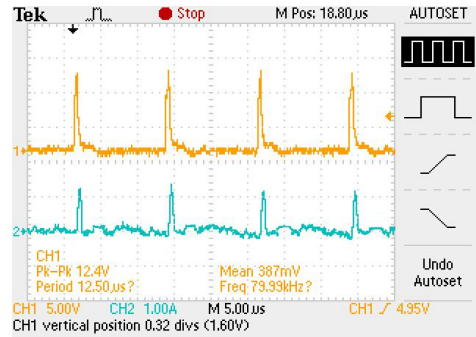


Fig.14. ZCS Operation in  $S_a$

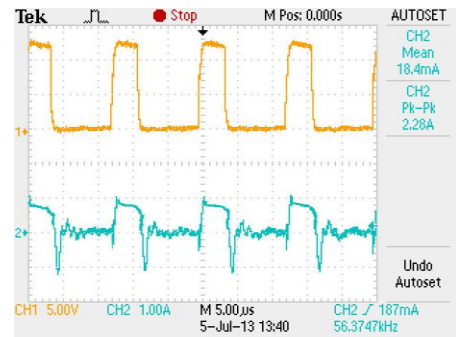


Fig.15. ZCS Operation in  $S_m$ .

## 6. Conclusion

The soft switching ZCS-PWM flyback dc/dc converter with a simple and compact configuration is simulated. The operation of this converter was analyzed. All semiconductor devices in the converter operate at ZCS turn on and off. The proposed converter is regulated by the conventional PWM technique at constant frequency. Therefore, the proposed ZCS-PWM flyback dc/dc converter combines the advantages of the PWM and ZCS techniques without additional current stresses compared to the conventional hard-switching method, improving converter performance and maintaining high efficiency. The simulation results show that the soft-switching PWM flyback converter results in better efficiency compared to conventional hard switching Flyback converter for the same power ratings. The simulation analysis carried out at both line and load regulation and the efficiency curve has been plotted for both the operation. It is noted that 12V regulated dc voltage is maintained at the output. High power efficiency 80-85% is acquired under different load and line condition for the proposed ZCS-PWM flyback dc/dc converter where conventional hard-switching converter shows efficiency 70-75% in simulation.



## 7. References

- [1] J. Y. Lee, "Single-stage AC/DC converter with input-current dead-zone control for wide input voltage ranges," IEEE Trans. Ind. Electron., vol. 54, no. 2, pp. 724–732, Apr. 2007.
- [2] N. Kasa, T. Iida, and L. Chen, "Flyback inverter controlled by sensorless current MPPT for photovoltaic power system," IEEE Trans. Ind. Electron., vol. 52, no. 4, pp. 1145–1152, Aug. 2005.
- [3] C. M. Wang, "Novel zero-voltage-transition PWM DC/DC converters," IEEE Trans. Ind. Electron., vol. 53, no. 1, pp. 254–262, Feb. 2006.
- [4] C. M. Wang, "New family of zero-current-switching PWM converters using a new zero-current-switching PWM auxiliary circuit," IEEE Trans. Ind. Electron., vol. 53, no. 3, pp. 768–777, Jun. 2006.
- [5] B. R. Lin and F. Y. Hsieh, "Soft-switching zeta-flyback converter with a buck-boost type of active clamp," IEEE Trans. Ind. Electron., vol. 54, no. 5, pp. 2813–2822, Oct. 2007.
- [6] N. P. Papanikolaou and E. C. Tatakis, "Active voltage clamp in flyback converters operating in CCM mode under wide load variation," IEEE Trans. Ind. Electron., vol. 51, no. 3, pp. 632–640, Jun. 2004.

IJERT